

# Graphene Q-switched Er,Yb:GdAl<sub>3</sub>(BO<sub>3</sub>)<sub>4</sub> laser at 1550 nm

KONSTANTIN GORBACHENYA,<sup>1</sup> VIKTOR KISEL,<sup>1</sup> ANATOLY YASUKEVICH,<sup>1</sup> PAVEL LOIKO,<sup>2</sup> XAVIER MATEOS,<sup>3,4,\*</sup> VIKTOR MALTSEV,<sup>5</sup> NIKOLAI LEONYUK,<sup>5</sup> MAGDALENA AGUILÓ,<sup>3</sup> FRANCESC DÍAZ,<sup>3</sup> UWE GRIEBNER,<sup>4</sup> VALENTIN PETROV,<sup>4</sup> AND NIKOLAI KULESHOV<sup>1</sup>

<sup>1</sup>Center for Optical Materials and Technologies, Belarusian National Technical University, 65/17 Nezavisimosti Ave., 220013 Minsk, Belarus

<sup>2</sup>ITMO University, Kronverkskiy pr., 49, 197101 Saint-Petersburg, Russia

<sup>3</sup>Física i Cristal·lografia de Materials i Nanomaterials (FICMA-FICNA), Universitat Rovira i Virgili (URV), Campus Sescelades, c/ Marcel·lí Domingo, s/n., E-43007 Tarragona, Spain

<sup>4</sup>Max Born Institute for Nonlinear Optics and Short Pulse Spectroscopy, Max-Born-Str. 2a, D-12489 Berlin, Germany

<sup>5</sup>Department of Crystallography and Crystal Chemistry, Moscow State University, 119992 GSP-2 Moscow, Russia

\*Corresponding author: [xavier.mateos@urv.cat](mailto:xavier.mateos@urv.cat), [mateos@mbi-berlin.de](mailto:mateos@mbi-berlin.de)

Received XX Month XXXX; revised XX Month, XXXX; accepted XX Month XXXX; posted XX Month XXXX (Doc. ID XXXXX); published XX Month XXXX

**A single-layer graphene saturable absorber is employed for passive Q-switching of an Er,Yb:GdAl<sub>3</sub>(BO<sub>3</sub>)<sub>4</sub> (Er,Yb:GdAB) compact laser, representing the first Er-doped oxoborate laser Q-switched by graphene. This laser is based on a c-cut 1.8 at.% Er<sup>3+</sup>, 15 at.% Yb<sup>3+</sup>:GdAB crystal diode-pumped at 0.976  $\mu\text{m}$ . It generates a maximum average output power of 360 mW at 1.55  $\mu\text{m}$  with a slope efficiency of 23% (with respect to the incident power). Stable  $\sim 1 \mu\text{J}$  / 130 ns pulses are achieved at a repetition rate of 400 kHz. This result represents the shortest pulse duration ever achieved in bulk Er lasers Q-switched by 2D-materials. Graphene is a promising material for generating nanosecond pulses at high repetition rates (MHz-range) in Er-doped oxoborate lasers emitting in the eye-safe range at 1.5-1.7  $\mu\text{m}$ .**

**OCIS codes:** (140.3070) Infrared and far-infrared lasers; (140.3540) Lasers, Q-switched; (140.3380) Laser materials.

<http://dx.doi.org/10.1364/AO.99.099999>

## 1. INTRODUCTION

The Erbium (Er<sup>3+</sup>) ion is attractive for eye-safe laser emission at 1.5-1.7  $\mu\text{m}$  originating from the <sup>4</sup>I<sub>13/2</sub>  $\rightarrow$  <sup>4</sup>I<sub>15/2</sub> transition. Erbium lasers are used in range-finding, telecom applications and medicine. A standard and simple approach to excite Er<sup>3+</sup> ions is to provide codoping of the host material with the (Er<sup>3+</sup>, Yb<sup>3+</sup>) couple [1]. The Yb<sup>3+</sup> ions can be efficiently pumped at  $\sim 0.98 \mu\text{m}$  by commercial and powerful InGaAs laser diodes. On condition of a proper Er<sup>3+</sup>/Yb<sup>3+</sup> codoping ratio and vibronic properties of the host (its phonon spectrum), the Yb<sup>3+</sup> ions can efficiently transfer part of their excitation energy to the Er<sup>3+</sup> ones, according to the <sup>2</sup>F<sub>5/2</sub> (Yb<sup>3+</sup>)  $\rightarrow$  <sup>4</sup>I<sub>11/2</sub> (Er<sup>3+</sup>) energy-transfer (ET) process [1,2], keeping low energy losses resulting from unwanted upconversion and back-energy-transfer processes.

Recently, the family of non-centrosymmetric trigonal rare-earth aluminium oxoborates, RAl<sub>3</sub>(BO<sub>3</sub>)<sub>4</sub> where R = Y, Gd, or Lu (shortly RAB), attracted a lot of attention for Yb<sup>3+</sup> doping [3] and (Er<sup>3+</sup>, Yb<sup>3+</sup>) codoping [2,4,5]. In the latter case, compared to the more standard

material, phosphate glass [1], the oxoborates offer much higher thermal conductivity of 7.7 and 6 W/mK along the *a* and *c*-axes, respectively [6], high efficiency of the Yb<sup>3+</sup> $\rightarrow$ Er<sup>3+</sup> ET ( $\eta_{\text{ET}} \sim 94\%$ ) [2] and weak upconversion due to the very short lifetime of the <sup>4</sup>I<sub>11/2</sub> excited-state,  $\sim 80$  ns [2], facilitated by high maximum phonon energy of the host,  $h\nu_{\text{max}} \sim 1500 \text{ cm}^{-1}$  [7] (here, the numbers given refer to YAB). Efficient continuous-wave (CW) Er,Yb:RAB lasers have been realized [2,4]. For example, a CW Er,Yb:YAB laser generated  $\sim 1$  W at 1.555  $\mu\text{m}$  with a slope efficiency of  $\eta = 35\%$  [2]. Recently, passively Q-switched (PQS) Er,Yb:RAB lasers have been reported using conventional "slow" saturable absorbers (SAs), e.g. Co<sup>2+</sup>:MgAl<sub>2</sub>O<sub>4</sub> spinel single-crystal [8, 9], as well as novel "fast" SAs - single-walled carbon nanotubes (SWCNTs) [10]. It should be noted that in [8-10], the generation of short pulses was facilitated by the use of microchip-like cavity design and, consequently, shortening of the cavity roundtrip time [11].

Graphene is on the rise in recent years as broadband SA for near-IR lasers [12]. It comprises a single layer of carbon atoms arranged in a

honeycomb lattice, and offers wavelength-independent absorption of  $\pi\alpha \sim 2.3\%$  (defined by the fine structure constant  $\alpha = e^2/\hbar c \approx 1/137$ ), broadband saturable absorption (1-3  $\mu\text{m}$ ), low saturation intensity  $I_{\text{sat}} \sim 1 \text{ MW/cm}^2$  for ns-long pulses, ultrafast recovery time and acceptable laser damage threshold [12,13]. Graphene can be deposited on various transparent dielectric materials leading to compact devices, e.g. when used in microchip lasers [14]. It should be noted that due to the specific band structure of graphene,  $I_{\text{sat}}$  increases with the photon energy  $h\nu$  [13], so that the use of graphene as a SA in lasers emitting at  $\sim 1.5\text{-}2 \mu\text{m}$  is advantageous as compared with the  $\sim 1 \mu\text{m}$  oscillators.

To date, graphene has been applied in multiple PQS  $\sim 1.5 \mu\text{m}$  Er fiber lasers, e.g. as in [15], while very few reports exist on Er bulk lasers of this type [16-18]. In these studies, the graphene-SA was implemented in in-band-pumped Er:YAG lasers emitting at 1617 and 1.645  $\mu\text{m}$  and producing relatively long (few  $\mu\text{s}$ ) pulses. In the present work, we report on the first realization of a graphene PQS (Er<sup>3+</sup>, Yb<sup>3+</sup>) codoped oxoborate laser as a concept for further development of microchip laser sources emitting ns-long pulses in the  $\sim 1.5 \mu\text{m}$  eye-safe spectral region with repetition rates in the MHz-range.

## 2. EXPERIMENTAL

### A. Laser crystal

The studied laser crystal had a composition of 1.8 at.% Er<sup>3+</sup>, 15 at.% Yb<sup>3+</sup>:GdAl<sub>3</sub>(BO<sub>3</sub>)<sub>4</sub> or shortly Er,Yb:GdAB ( $N_{\text{Er}} = 1.0$  and  $N_{\text{Yb}} = 8.3 \times 10^{20} \text{ cm}^{-3}$ , crystal density  $\rho = 4.34 \text{ g/cm}^3$ ). The crystal was grown by the dipping seeded high-temperature solution growth method at a cooling rate of 0.2-0.5  $^{\circ}\text{C/day}$  in the temperature range of 1060-1000  $^{\circ}\text{C}$  using K<sub>2</sub>Mo<sub>3</sub>O<sub>10</sub>-based flux [19] and is shown in Fig. 1(a). The chosen Er<sup>3+</sup>/Yb<sup>3+</sup> codoping ratio provided an efficiency for the Yb<sup>3+</sup>  $\rightarrow$  Er<sup>3+</sup> ET of  $\eta_{\text{ET}} > 90\%$ ; at the same time, the high Yb<sup>3+</sup> doping level favored high pump absorption. The GdAB crystal belongs to the trigonal system (space group R32, point group 32), optically uniaxial (the optical axis is parallel to the *c*-axis). Its optical properties are characterized for two principal light polarizations,  $\mathbf{E} \parallel \mathbf{c}$  ( $\pi$ ) and  $\mathbf{E} \perp \mathbf{c}$  ( $\sigma$ ).

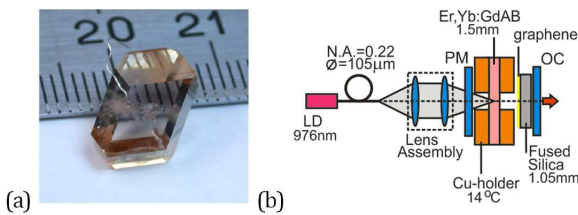


Fig. 1. (a) Photo of the as-grown Er,Yb:GdAB crystal; (b) scheme of the compact diode-pumped graphene PQS Er,Yb:GdAB laser: LD – laser diode, PM – pump mirror, OC – output coupler.

The relevant transition cross-sections for Yb<sup>3+</sup> and Er<sup>3+</sup> ions in GdAB are shown in Fig. 2. For the  ${}^2F_{7/2} \rightarrow {}^2F_{5/2}$  transition of Yb<sup>3+</sup>, a strong anisotropy of the absorption cross-sections,  $\sigma_{\text{abs}}$ , is observed, Fig. 2(a). For  $\sigma$ -polarization, the maximum  $\sigma_{\text{abs}} = 3.5 \times 10^{-20} \text{ cm}^2$  occurs at 0.9764  $\mu\text{m}$ ; the full width at half maximum (FWHM) of the absorption band is 17.6 nm. For  $\pi$ -polarization, the maximum  $\sigma_{\text{abs}}$  is  $\sim 11$  times lower. Thus, *c*-cut Er,Yb:GdAB crystal is preferable to ensure highest absorption with unpolarized pump sources. The absorption,  $\sigma_{\text{abs}}$ , and stimulated-emission (SE),  $\sigma_{\text{SE}}$ , cross-section

spectra for the  ${}^4I_{15/2} \leftrightarrow {}^4I_{13/2}$  transition of the quasi-three level Er<sup>3+</sup> laser are shown in Fig. 2(b) for  $\sigma$ -polarization which is the only one accessible for a *c*-cut crystal. At a wavelength of  $\sim 1.55 \mu\text{m}$ , which corresponds to a local peak in the SE cross-section spectra  $\sigma_{\text{SE}}$  is  $0.6 \times 10^{-20} \text{ cm}^2$ . It should be noted that the choice of the Er,Yb:GdAB crystal for PQS laser experiments is based on its beneficial spectroscopic properties as compared with its (Er<sup>3+</sup>, Yb<sup>3+</sup>) codoped YAB and LuAB counterparts [4], namely higher  $\sigma_{\text{abs}}$  for the Yb<sup>3+</sup> ion and longer lifetime of the upper laser level for Er<sup>3+</sup> ( $\tau({}^4I_{13/2}) = 350 \mu\text{s}$ ).

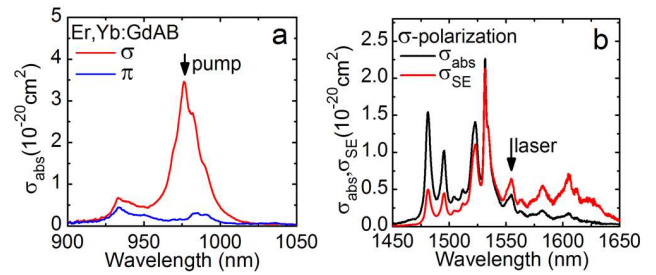


Fig. 2. Spectroscopy of Er,Yb:GdAB: (a) absorption cross-sections,  $\sigma_{\text{abs}}$ , for the  ${}^2F_{7/2} \rightarrow {}^2F_{5/2}$  transition of Yb<sup>3+</sup> for  $\pi$  and  $\sigma$  light polarizations; (b) absorption,  $\sigma_{\text{abs}}$ , and stimulated-emission,  $\sigma_{\text{SE}}$ , cross-sections for the  ${}^4I_{15/2} \leftrightarrow {}^4I_{13/2}$  transition of Er<sup>3+</sup> for  $\sigma$  light polarization; the arrows indicate the pump and laser wavelengths.

### B. Laser set-up

The scheme of the graphene PQS Er,Yb:GdAB laser is shown in Fig. 1(b). The laser element was 1.5 mm-thick. Both surfaces of the element were polished to laser quality and antireflection (AR) coated at  $\sim 0.98$  and  $\sim 1.55 \mu\text{m}$ . The element was wrapped in indium foil and mounted between two copper slabs with a hole in the center to permit passing the pump and laser beams. Its temperature was kept at 14  $^{\circ}\text{C}$  by a Peltier element with a water-cooled heat sink.

The laser cavity consisted of a flat pump mirror (PM) that was AR-coated for 0.95–1.05  $\mu\text{m}$  and high-reflection (HR) coated for 1.5–1.6  $\mu\text{m}$ , and a flat output coupler (OC) with a transmittance of  $T_{\text{OC}} = 9\%$  at  $\sim 1.55 \mu\text{m}$ . This OC was chosen as it ensured stable passive Q-switching. The crystal was pumped by a fiber-coupled InGaAs laser diode (fiber core diameter: 105  $\mu\text{m}$ , N.A.: 0.22) emitting unpolarized radiation at 0.976  $\mu\text{m}$ . The pump beam was reimaged into the crystal by a lens assembly providing a pump waist of  $w_p = 60 \mu\text{m}$  and a confocal parameter  $2z_R = 1.0 \text{ mm}$  ( $M^2 = 42$  for the pump beam). The measured small-signal pump absorption of the crystal was  $\sim 90\%$ .

A commercial transmission-type graphene-SA was inserted between the laser element and the OC. The total geometrical length of the cavity  $L_{\text{cav}}$  was 7.5 mm, limited by the design of the crystal holder. The minimum cavity length was used in order to shorten the cavity roundtrip time. The laser output was detected with a fast InGaAs photodetector (New Focus) and a 500 MHz digital oscilloscope (Tektronix TDS-3052B).

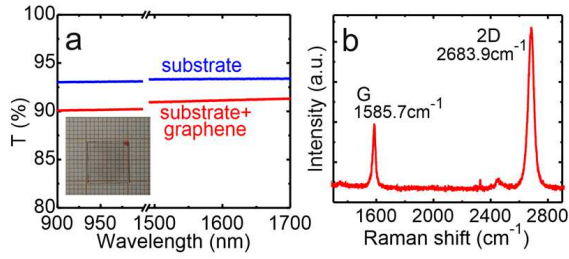


Fig. 3. Graphene-SA: (a) small-signal transmission spectrum, *inset* – image of the SA; (b) Raman spectrum,  $\lambda_{\text{exc}} = 0.514 \mu\text{m}$ .

The graphene-SA was synthesized by the Chemical Vapor Deposition (CVD) method. The SA consisted of a 1.05 mm-thick uncoated fused silica substrate and a single layer of carbon atoms. At  $\sim 1.55 \mu\text{m}$ , the small-signal internal absorption of graphene was  $\alpha'_{\text{SA}} = 1 - T_{\text{SA}} = 2.5\%$ , where  $T_{\text{SA}} = T(\text{graphene} + \text{substrate}) / T(\text{substrate})$ , see Fig. 3(a). The number of carbon layers ( $n = 1$ ) was confirmed by Raman spectroscopy [20] indicating a ratio of the integrated areas of 2D and G bands of  $\sim 4$ , Fig. 3(b). The saturation intensity of the graphene-SA was  $I_{\text{sat}} \sim 1 \text{ MW/cm}^2$ , the modulation depth  $\alpha'_s = 0.12\%$  (as estimated from the fraction of the saturable losses,  $\alpha'_s/\alpha'_{\text{SA}} = 0.05$ ) [21] and the fast and slow recovery times of the initial absorption  $\tau_{\text{rec1}} = 0.25 \text{ ps}$  and  $\tau_{\text{rec2}} = 1.16 \text{ ps}$ , respectively.

### 3. RESULTS AND DISCUSSION

Laser operation with a c-cut Er,Yb:GdAB in a plano-plano cavity is an indication of a positive thermal lens. According to [22], we estimate its sensitivity factor,  $M = dD/dP_{\text{abs}}$ , as  $46 \text{ m}^{-1}/\text{W}$ , using the data reported for the isostructural YAB crystal. This sensitivity factor corresponds to a variation of the focal length of the thermal lens of 6–10 mm for the utilized range of pump powers. By using these values in the ABCD-modelling, we derived the radius of the laser mode in the laser crystal and on the SA as  $w_L = 55 \pm 5 \mu\text{m}$ .

Stable passive Q-switching of the Er,Yb:GdAB laser was obtained with the graphene-SA. This laser generated a maximum average output power of 360 mW with a slope efficiency of  $\eta = 23\%$  (with respect to the incident pump power  $P_{\text{inc}}$ ), Fig. 4(a). The laser threshold was at  $P_{\text{inc}} = 3.4 \text{ W}$  and the optical-to-optical efficiency  $\eta_{\text{opt}}$  amounted to 7%. The power scaling of the PQS laser was limited by degradation of the graphene-SA at  $P_{\text{inc}} > 5 \text{ W}$  that can be attributed to the absorption of the residual (non-absorbed) pump in the SA, cf. Fig. 3(a). In the CW mode (removing the SA from the cavity) the laser generated a maximum output power of 510 mW at the same  $P_{\text{inc}}$ , so that a relatively high Q-switching conversion efficiency of  $\eta_{\text{conv}} = 70\%$  was achieved. In both regimes, CW and PQS, the laser emission was unpolarized and appeared at  $\sim 1.550 \mu\text{m}$ , as shown in Fig. 4(b). The spatial profile of the output laser beam was nearly-circular, see inset in Fig. 4(a), and the measured  $M^2$  parameter was less than 1.5.

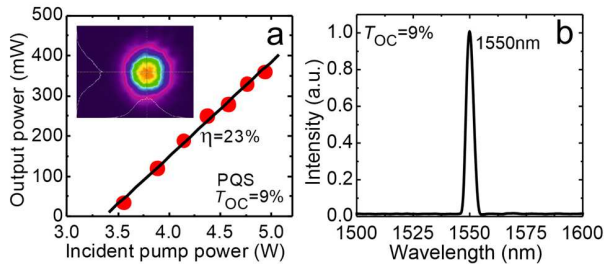


Fig. 4. Graphene PQS Er,Yb:GdAB laser: (a) input-output dependence,  $\eta$  – slope efficiency, *inset* – 2D profile of the output beam; (b) typical laser emission spectrum,  $P_{\text{inc}} = 4.9 \text{ W}$ .

With the increase of  $P_{\text{inc}}$ , the pulse duration  $\Delta\tau$  (determined as FWHM) shortened from 240 to 130 ns. This was accompanied by an increase of the PRF in the 240–400 kHz range and an increase of the pulse energy  $E_{\text{out}} = P_{\text{out}}/\text{PRF}$  in the 0.5–0.9  $\mu\text{J}$  range, see Fig. 5(a-c). Consequently, the peak power of the PQS laser  $P_{\text{peak}} = E_{\text{out}}/\Delta\tau$  reached 6.9 W, Fig. 5(d). The dependence of the pulse characteristics on pump power in graphene PQS lasers is determined by the variation of the bleaching of the SA with pump power as described previously [23]. In our case, the peak on-axis intracavity intensity on the SA amounts to  $\sim 4.7 \text{ MW/cm}^2$  which means complete bleaching of the SA. It was calculated as  $I_{\text{in}} = X[2E_{\text{out}}/\pi w_L^2 \Delta\tau^*]$ , where  $X = (2 - T_{\text{oc}})/(T_{\text{oc}})$  [24], the term “2” indicates a Gaussian spatial profile of the laser mode and  $\Delta\tau^* \approx 1.06 \cdot \Delta\tau$  is the effective pulse duration.

The oscilloscope trace of the single Q-switched pulse recorded at the maximum  $P_{\text{inc}} = 4.9 \text{ W}$  is shown in Fig. 6(a). The corresponding pulse train, Fig. 6(b), indicates very low intensity instabilities ( $< 5\%$ ) and pulse-to-pulse timing jitter with an rms value  $< 7\%$ .

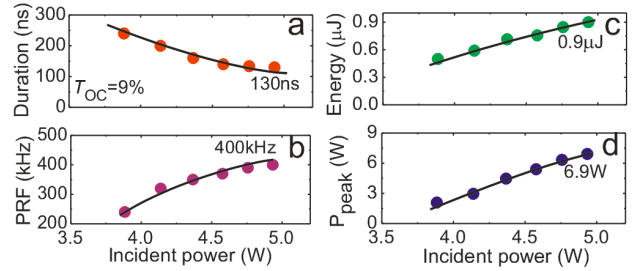


Fig. 5. Graphene PQS Er,Yb:GdAB laser: pulse duration  $\Delta\tau$  (FWHM) (a), pulse repetition frequency (PRF) (b), pulse energy  $E_{\text{out}} = P_{\text{out}}/\text{PRF}$  (c), and peak power  $P_{\text{peak}} = E_{\text{out}}/\Delta\tau$  (d).

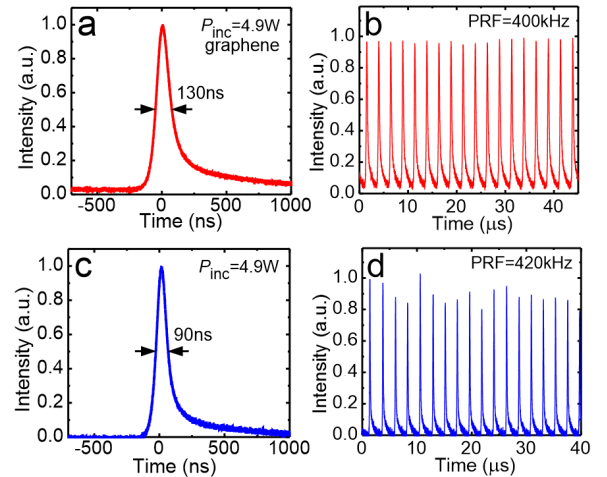


Fig. 6. Oscilloscope traces of the single Q-switched pulse (a,c) and the corresponding pulse trains (b,d) from the graphene PQS Er,Yb:GdAB laser using the 1.8 at.% Er<sup>3+</sup>, 15 at.% Yb<sup>3+</sup> doped (a,b) or 1.0 at.% Er<sup>3+</sup>, 11 at.% Yb<sup>3+</sup> doped (c,d) crystal,  $P_{\text{inc}} = 4.9 \text{ W}$ .

Previously, graphene-SA has been employed for PQS of multiple fiber Er lasers, e.g. see [15] where such a laser generated 1.1 mW at 1.566  $\mu\text{m}$  corresponding to 16.7 nJ / 3.7  $\mu\text{s}$  pulses at PRF = 66 kHz. Regarding bulk Er lasers, see Table 1, graphene-SA was used in PQS oscillators based on single-crystal or ceramic Er:YAG under in-band-pumping [16-18,25]. Due to the use of long cavities with a large mode size in the crystal, these oscillators provided pulse durations of few  $\mu\text{s}$  and energies of 6...13  $\mu\text{J}$ . The results achieved in the present work are superior to the previous publications on graphene PQS Er bulk lasers in terms of  $\Delta\tau$  due to the use of a microchip-type set-up. The value of  $E_{\text{out}}$  achieved in the present work is lower than in [16-18] due to a smaller mode size for the utilized laser configuration and the shorter energy storage time for Er:Yb:GdAB (350  $\mu\text{s}$ ) as compared with that of Er:YAG (~5 ms).

As a first step towards monolithic Er true microchip lasers PQS with a graphene-SA, an additional experiment was performed by using a 1 mm-thick *c*-cut 1.0 at.% Er<sup>3+</sup>, 11 at.% Yb<sup>3+</sup>:GdAB crystal with the PM deposited directly on one of the crystal faces. It provided HR ( $R > 99.5\%$ ) at 1.550  $\mu\text{m}$  and high transmission ( $T > 95\%$ ) at 0.976  $\mu\text{m}$ . The second face was AR-coated for 0.9-1.0 and for 1.5-1.6  $\mu\text{m}$ . The crystal was studied in the same set-up as shown in Fig. 1(b). The use of this crystal allowed us to reduce substantially the total geometrical cavity length to ~4 mm.

**Table 1. Output Characteristics of Previously Reported Bulk 1.5 - 1.7  $\mu\text{m}$  Er-doped Lasers PQS by Graphene-SA**

Laser material	$P_{\text{out}}$ mW	$\lambda_L$ nm	$E_{\text{out}}$ $\mu\text{J}$	$\Delta\tau$ ns	PRF, kHz	Ref.
Er:Yb:GdAB	360	1550	0.9	130	400	This work
Er:YAG ceramic	528	1645	7.1	1490	75	[16]
Er:YAG	480	1645	13.5	7780	36	[17]
Er:YAG ceramic	662	1617	12.2	1900	54	[18]
Er:LuYAG	460	1648	5.8	2050	79	[25]

Using such a quasi-monolithic set-up, we achieved a maximum average output power of 420 mW at 1.55  $\mu\text{m}$  (PQS operation mode) for  $P_{\text{inc}} = 4.9$  W. The shortest pulse duration was 90 ns corresponding to a pulse energy of ~1  $\mu\text{J}$  and a PRF of 420 kHz, see Fig. 6(c). In consequence, the peak power reached 11 W. However, the stability of the pulse train was deteriorated in comparison with the previous case. We attribute this unsatisfactory stability to a large extent to the non-absorbed pump, heating the SA as the laser crystal had lower Yb<sup>3+</sup> concentration (the measured small-signal pump absorption was ~75%). This problem can be easily resolved by coating the second crystal face HR for the pump.

The advantage of graphene as a SA is its broadband saturable absorption [13]. In Fig. 7, we plotted the pulse duration  $\Delta\tau$  and pulse energy  $E_{\text{out}}$  of compact graphene PQS lasers based on Yb<sup>3+</sup> [21,26], Er<sup>3+</sup>, Tm<sup>3+</sup> [14,23] or Ho<sup>3+</sup> [27] ions emitting in the 1.0-2.1  $\mu\text{m}$  spectral range reported so far. By comparing the results for single-layer ( $n = 1$ ) and multi-layer ( $n = 3$ ) graphene-SAs at a fixed laser wavelength, it becomes clear that the increase of  $n$  is beneficial for the pulse characteristics. The latter is due to the increased modulation depth of the SA. However, for large  $n$  ( $n > 3$ ), this advantage is mitigated by the rise of scattering at the layer-to-layer interfaces [13,27].

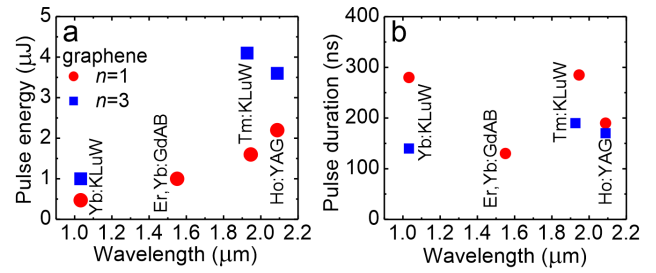


Fig. 7. Pulse energy (a) and pulse duration (b) achieved in compact graphene PQS near-IR bulk lasers based on Yb<sup>3+</sup> [21,26], Er<sup>3+</sup> (this work), Tm<sup>3+</sup> [14,23] or Ho<sup>3+</sup> [27] ions,  $n$  is the number of carbon layers in the graphene-SA. KLuW: KLu(WO<sub>4</sub>)<sub>2</sub> is a monoclinic biaxial host.

From Fig. 7, one can conclude that with the red-shift of the emission wavelength,  $E_{\text{out}}$  tends to increase and  $\Delta\tau$  to shorten. Physically this is related to two reasons. First,  $I_{\text{sat}}$  of graphene decreases for lower photon energies  $h\nu$ , leading to easier bleaching of the SA. Second, the fraction of the saturable loss  $\alpha'_s/\alpha'_{\text{SA}}$  increases due to the reduced light scattering resulting in larger modulation depth [26].

#### 4. CONCLUSION

We report on the first realization of a graphene PQS erbium oxoborate laser at ~1.5  $\mu\text{m}$ . Using an Er:Yb:GdAB crystal pumped by an InGaAs diode at 0.976  $\mu\text{m}$ , a maximum average output power of 360 mW is extracted at 1.550  $\mu\text{m}$  (eye-safe region) corresponding to a slope efficiency of 23%. Laser pulses of ~1  $\mu\text{J}$  energy and 130 ns duration are generated at a repetition frequency of 400 kHz. These are the shortest pulses ever achieved from an Er-doped bulk laser PQS by carbon nanostructures which is mainly attributed to the use of a microchip-type set-up. Further shortening of the pulse duration and increasing of the pulse energy can be expected by a direct coating of graphene on the HR/AR coated exit crystal face and a reduction of the cavity length, as well as using a SA containing several (e.g.,  $n = 3$ ) carbon layers to increase the modulation depth. We expect that these improvements may lead to the generation of sub-100 ns pulses with energies reaching ~10  $\mu\text{J}$ . By power scaling of the Er:Yb:GdAB laser PQS by graphene SAs one can potentially reach the MHz PRF range.

**Funding.** Spanish Government (MAT2016-75716-C2-1-R, (AEI/FEDER/UE), MAT2013-47395-C4-4-R, TEC 2014-55948-R); Generalitat de Catalunya (2014SGR1358).

**Acknowledgment.** F.D. acknowledges additional support through the ICREA academia award 2010/ICREA-02 for excellence in research. This work has received funding from the European Union's Horizon 2020 research and innovation programme under the Marie Skłodowska-Curie grant agreement No 657630. P.L. acknowledges financial support from the Government of the Russian Federation (Grant 074-U01) through ITMO Post-Doctoral Fellowship scheme.

#### References

1. G. Karlsson, F. Laurell, J. Tellefsen, B. Denker, B. Galagan, V. Osiko, and S. Sverchok, "Development and characterization of Yb-Er laser glass for high average power laser diode pumping," *Appl. Phys. B* **75**(1), 41–46 (2002).

2. N. A. Tolstik, S. V. Kurilchik, V. E. Kisel, N. V. Kuleshov, V. V. Maltsev, O. V. Pilipenko, E. V. Koporulina, and N. I. Leonyuk, "Efficient 1 W continuous-wave diode-pumped Er,Yb:YAl<sub>3</sub>(BO<sub>3</sub>)<sub>4</sub> laser," *Opt. Lett.* **32**(22), 3233–3235 (2007).
3. J. Liu, X. Mateos, H. Zhang, J. Li, J. Wang, and V. Petrov, "High-power laser performance of Yb:YAl<sub>3</sub>(BO<sub>3</sub>)<sub>4</sub> crystals cut along the crystallographic axes," *IEEE J. Quant. Electron.* **43**(5), 385–390 (2007).
4. K. N. Gorbachenya, V. E. Kisel, A. S. Yasukevich, V. V. Maltsev, N. I. Leonyuk, and N. V. Kuleshov, "Highly efficient continuous-wave diode-pumped Er,Yb:GdAl<sub>3</sub>(BO<sub>3</sub>)<sub>4</sub> laser," *Opt. Lett.* **38**(14), 2446–2448 (2013).
5. Y. Chen, Y. Lin, J. Huang, X. Gong, Z. Luo, and Y. Huang, "Spectroscopic and laser properties of Er<sup>3+</sup>:Yb<sup>3+</sup>:LuAl<sub>3</sub>(BO<sub>3</sub>)<sub>4</sub> crystal at 1.5–1.6 μm," *Opt. Express* **18**(13), 13700–13707 (2010).
6. N. A. Tolstik, G. Huber, V. V. Maltsev, N. I. Leonyuk, and N. V. Kuleshov, "Excited state absorption, energy levels, and thermal conductivity of Er<sup>3+</sup>:YAB," *Appl. Phys. B* **92**(4), 567–571 (2008).
7. D. Jaque, M. O. Ramirez, L. E. Bausa, J. G. Sole, E. Cavalli, A. Spheghini, and M. Betinelli, "Nd<sup>3+</sup> → Yb<sup>3+</sup> energy transfer in the YAl<sub>3</sub>(BO<sub>3</sub>)<sub>4</sub> nonlinear laser crystal," *Phys. Rev. B* **68**(3), 035118–1–9 (2003).
8. V. E. Kisel, K. N. Gorbachenya, A. S. Yasukevich, A. M. Ivashko, N. V. Kuleshov, V. V. Maltsev, and N. I. Leonyuk, "Passively Q-switched microchip Er,Yb:YAl<sub>3</sub>(BO<sub>3</sub>)<sub>4</sub> diode-pumped laser," *Opt. Lett.* **37**(13), 2745–2747 (2012).
9. K. N. Gorbachenya, V. E. Kisel, A. S. Yasukevich, V. V. Maltsev, N. I. Leonyuk, and N. V. Kuleshov, "Eye-safe 1.55 μm passively Q-switched Er,Yb:GdAl<sub>3</sub>(BO<sub>3</sub>)<sub>4</sub> diode-pumped laser," *Opt. Lett.* **41**(5), 918–921 (2016).
10. K. N. Gorbachenya, V. E. Kisel, A. S. Yasukevich, M. B. Prudnikova, V. V. Maltsev, N. I. Leonyuk, S. Y. Choi, F. Rotermund, and N. V. Kuleshov, "Passively Q-switched Er,Yb:GdAl<sub>3</sub>(BO<sub>3</sub>)<sub>4</sub> laser with single-walled carbon nanotube based saturable absorber" *Laser Phys. Lett.* **14**(3), 035802–1–5 (2017).
11. J. J. Zayhowski and C. Dill, "Diode-pumped passively Q-switched picosecond microchip lasers," *Opt. Lett.* **19**(18), 1427–1429 (1994).
12. Q. Bao, H. Zhang, Y. Wang, Z. Ni, Y. Yan, Z. X. Shen, K. P. Loh, and D. Y. Tang, "Atomic-layer graphene as a saturable absorber for ultrafast pulsed lasers," *Adv. Funct. Mater.* **19**(19), 3077–3083 (2009).
13. F. Zhang, S. Han, Y. Liu, Z. Wang, and X. Xu, "Dependence of the saturable absorption of graphene upon excitation photon energy," *Appl. Phys. Lett.* **106**(9), 091102–1–5 (2015).
14. J. M. Serres, P. Loiko, X. Mateos, K. Yumashev, U. Griebner, V. Petrov, M. Aguiló, and F. Díaz, "Tm:KLu(WO<sub>4</sub>)<sub>2</sub> microchip laser Q-switched by a graphene-based saturable absorber," *Opt. Express* **23**(11), 14108–14113 (2015).
15. Z. Luo, M. Zhou, J. Weng, G. Huang, H. Xu, C. Ye, and Z. Cai, "Graphene-based passively Q-switched dual-wavelength erbium-doped fiber laser," *Opt. Lett.* **35**(21), 3709–3711 (2010).
16. Z. X. Zhu, Y. Wang, H. Chen, H. T. Huang, D. Y. Shen, J. Zhang, and D. Y. Tang, "A graphene-based passively Q-switched polycrystalline Er:YAG ceramic laser operating at 1645 nm," *Laser Phys. Lett.* **10**(5), 055801–1–4 (2013).
17. R. Zhou, P. Tang, Y. Chen, S. Chen, C. Zhao, H. Zhang, and S. Wen, "Large-energy, narrow-bandwidth laser pulse at 1645 nm in a diode-pumped Er:YAG solid-state laser passively Q-switched by a monolayer graphene saturable absorber," *Appl. Opt.* **53**(2), 254–258 (2014).
18. X. Zhang, J. Liu, D. Shen, X. Yang, D. Tang, and D. Fan, "Efficient graphene Q-switching of an in-band pumped polycrystalline Er:YAG ceramic laser at 1617 nm," *IEEE Photon. Technol. Lett.* **25**(13), 1294–1296 (2013).
19. V. V. Maltsev, E. V. Koporulina, N. I. Leonyuk, K. N. Gorbachenya, V. E. Kisel, A. S. Yasukevich, and N. V. Kuleshov, "Crystal growth of CW diode-pumped (Er<sup>3+</sup>, Yb<sup>3+</sup>):GdAl<sub>3</sub>(BO<sub>3</sub>)<sub>4</sub> laser material," *J. Cryst. Growth* **401**, 807–812 (2014).
20. A. C. Ferrari, J. C. Meyer, V. Scardaci, C. Casiraghi, M. Lazzeri, F. Mauri, S. Piscanec, D. Jiang, K. S. Novoselov, S. Roth, and A. K. Geim, "Raman spectrum of graphene and graphene layers," *Phys. Rev. Lett.* **97**(18), 187401–1–4 (2006).
21. P. A. Loiko, J. M. Serres, X. Mateos, J. Liu, H. Zhang, A. S. Yasukevich, K. V. Yumashev, V. Petrov, U. Griebner, M. Aguiló, and F. Díaz, "Passive Q-switching of Yb bulk lasers by a graphene saturable absorber," *Appl. Phys. B* **122**(4), 105–1–8 (2016).
22. P. A. Loiko, V. V. Filippov, N. V. Kuleshov, N. I. Leonyuk, V. V. Maltsev, and K. V. Yumashev, "Thermo-optic characterization of Yb:YAl<sub>3</sub>(BO<sub>3</sub>)<sub>4</sub> laser crystal," *Appl. Phys. B* **117**(2), 577–583 (2014).
23. A. S. Yasukevich, P. Loiko, N. V. Gusakova, J. M. Serres, X. Mateos, K. V. Yumashev, N. V. Kuleshov, V. Petrov, U. Griebner, M. Aguiló, and F. Díaz, "Modeling of graphene Q-switched Tm lasers," *Opt. Commun.* **389**, 15–22 (2017).
24. S. Chénais, F. Balembois, F. Druon, G. Lucas-Leclin, and P. Georges, "Thermal lensing in diode-pumped Ytterbium lasers - part II: evaluation of quantum efficiencies and thermo-optic coefficients," *IEEE J. Quantum Electron.* **40**(9), 1235–1243 (2004).
25. X. F. Yang, Y. Wang, H. T. Huang, D. Y. Shen, D. Y. Tang, H. Y. Zhu, X. D. Xu, D. H. Zhou, and J. Xu, "A passively Q-switched Er:LuYAG laser with a graphene saturable absorber," *Laser Phys. Lett.* **10**(10), 105810–1–4 (2013).
26. J. M. Serres, P. Loiko, X. Mateos, H. Yu, H. Zhang, Y. Chen, V. Petrov, U. Griebner, K. Yumashev, M. Aguiló, and F. Díaz, "MoS<sub>2</sub> saturable absorber for passive Q-switching of Yb and Tm microchip lasers," *Opt. Mater. Express* **6**(10), 3262–327 (2016).
27. R. Lan, P. Loiko, X. Mateos, Y. Wang, J. Li, Y. Pan, S. Y. Choi, M. H. Kim, F. Rotermund, A. Yasukevich, K. Yumashev, U. Griebner, and V. Petrov, "Passive Q-switching of microchip lasers based on Ho:YAG ceramic," *Appl. Opt.* **55**(18), 4877–4887 (2016).